Experimental testing and analytical modelling of Skylark floor beams

Dr. Gabriele Granello

May 16, 2023

Abstract

In the first part of the paper, the main results of a series of experiments focused on Skylark floor beams are presented. Eight Skylark floor beam specimens were tested in a 4-point bending configuration. Specimens showed a ductile failure because of reaching the compression capacity of the stitched joints. In the second part, an analytical model to calculate the beam capacity and deflection is presented. Comparison with the experimental results show that the analytical model appears suitable for design purposes.

1 Experimental testing

1.1 Experimental setup

Five M beam specimens and three L beam specimens were tested in 4-point bending (Figure 1). M specimens had a span of 5.1 m (column centre to column centre), and were 350 mm high and 600 mm wide. L specimens had the same section but spanning 5.7 m (column centre to column centre).

The load exerted by the hydraulic actuator was applied to the timber beams by using a 1.7 m long UC 203 x 203 x 71 mm steel profile and two 10 x 500 x 800mm steel plates. Two 40mm diameter steel bars were welded to the plates to create a pin connection between the load spreading beam and the timber specimens. The plates were positioned so that the forces push on the timber specimen at plus/minus 1.7 m from the centre of the beam.

The following instrumentation was installed for data acquisition:

- Linear transducers (potentiometers) were used to track the specimen displacement profile. Five of them were mounted to measure the beam's vertical deflection, while two of them were mounted to measure the gap opening between the beam and the column.
- A 250 kN-capacity load cell was used to measure the actuator force.
- Two high resolution cameras were used to track the strain profile by using digital image correlation. Since the cameras' configuration geometry allows them to

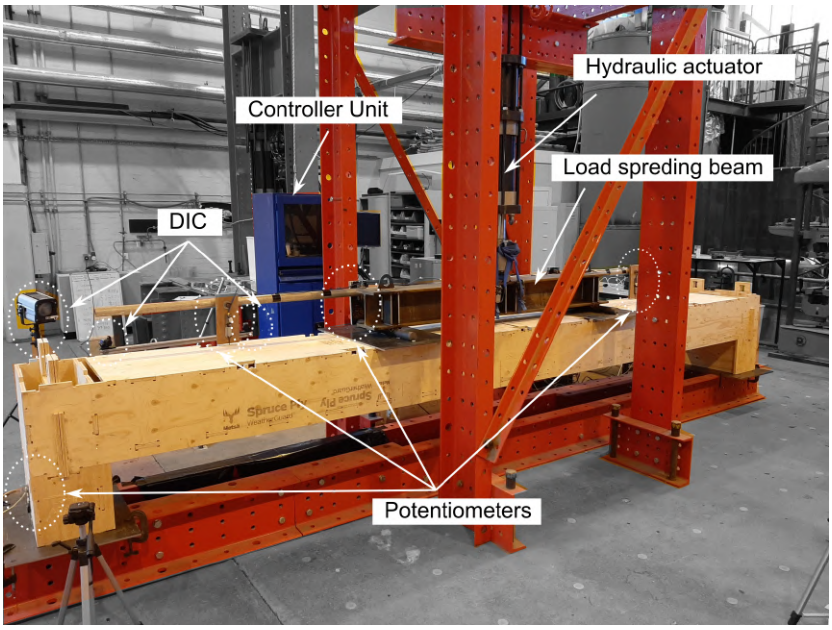

Figure 1: Experimental setup.

focus on roughly a 1.5 m length of the specimen, their positions were changed between tests.

The loading protocol approximately follows the guidance given in EN 1380:2009 [1] for connectors in timber structures. Although the test is for a complete element rather than a connection, its response is driven by local behaviour at connections between parts, and the cycle of loading recommended in that testing standard was used to capture the different stiffness of the system under initial loading, and the unload-reload cycle. The test was carried out in displacement control, with the actuator moving at 3 mm per minute. The loading protocol consisted of a monotonic ramp of 22 mm (roughly span divided by 250), a one minute hold, a monotonic ramp back to 5 mm, a one minute hold, and then a monotonic ramp until failure.

1.2 Failure mechanism

The weakest point of both the M and L specimens was found in the web's dovetail joint (Figure 2 and 3).

The specimen failure was initiated in the stitched joint, where local compressive failure occurred at the contact between the tab on the bottom flange and the web, as reported in the figure below. In addition to the stitched joints, damage was also observed in the dovetail joints, especially the joint placed at the bottom flange of the specimens.

It can also be observed that the joint panel opened a gap with the mock column, while no column uplift was identified during the test. This suggests the joint behaves

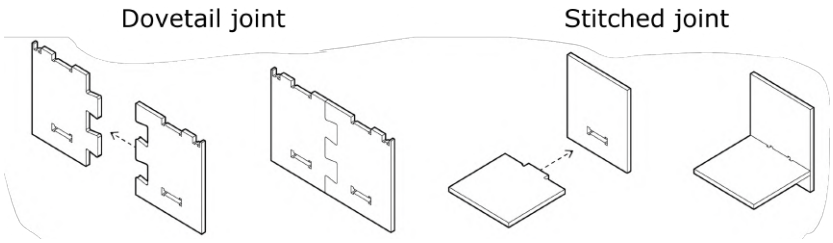

Figure 2: Dovetail joint vs stitched joint.

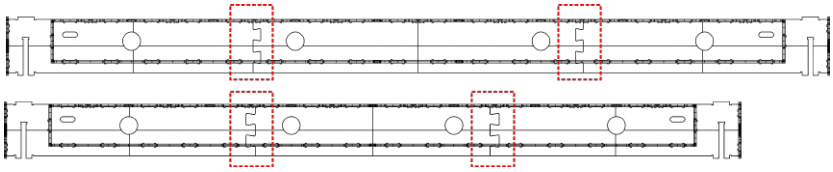

Figure 3: Locations where the failure initiated.

as a pin, i.e. the shear panel can only transfer a negligible (if any) amount of bending moment to the column.

Figure 4: a) Overview, b) detail of stitch joints and side dovetail joints, c) detail of bottom flange dovetail joint.

1.3 Failure load

All M specimens failed in a ductile manner: the specimens were able to maintain the load for a while after reaching the peak force. The response of the specimens in terms of force (exerted by the actuator) vs mid-span displacement is reported in the graph and table below. The peak force occurred between 21.3 kN and 24.9 kN, depending on the specimen.

L specimens showed less ductility than M specimens. That was because the web panels started to fall out of plane after the yielding of the stitched joints. The response of the specimens in terms of force (exerted by the actuator) vs mid-span displacement is reported in the graph and table below. The peak force occurred between 19.3 kN and 25.8 kN, depending on the specimen.

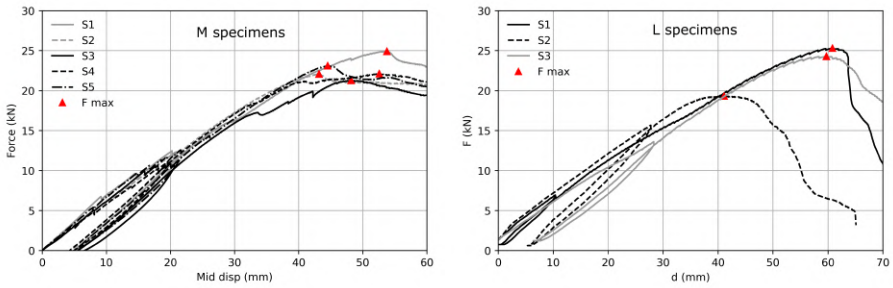

Figure 5: Force-displacement curve for the specimens.

The experimental results in terms of capacity are reported in table 1 for the M specimens, and table 2 for the L specimens.

Table 1: Experimental results of the M specimens.

Specimen	**Material**	F_{max} **(kN)**	$M_{j,max}$ **(kNm)**
S1-M	Metsa spruce plywood	24.9	20.9
S2-M	Metsa spruce plywood	22.1	18.5
S3-M	Metsa spruce plywood	21.3	17.8
S4-M	Metsa spruce plywood	22.1	18.5
S5-M	Metsa spruce plywood	23.1	19.3
			19.0

Table 2: Experimental results of the L specimens.

Specimen	**Material**	F_{max} **(kN)**	$M_{j,max}$ **(kNm)**
S1-L	Metsa spruce plywood	25.8	21.8
S2-L	Metsa spruce plywood	19.3*	16.3*
S3-L	Metsa spruce plywood	24.3	20.6
* failed prematurely			21.2

1.4 Joint stiffness

The relative rotation occurring in the castellated joint was estimated by using the horizontal differential displacements across the joint itself measured by using Digital Image Correlation. Specifically, the differential displacements in 3 points along the section depth were fitted with a linear function so that the slope represents an estimate of the relative rotation.

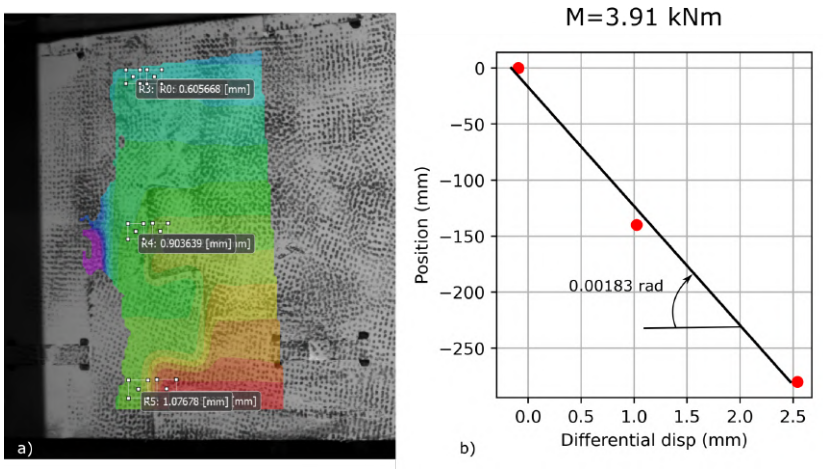

Figure 6: a) Extraction of the horizontal displacements in the representative points. b) Fitting of the differential displacements to estimate the relative rotation.

The moment rotation relationship of the joint is then reported in Figure 7 . It can be seen that the relationship appears to be linear until the moment reaches 7.5 kNm. The elastic initial rotational stiffness k_R calculated between 10% and 40% of the peak value of the moment is equal to 2295 kNm/rad

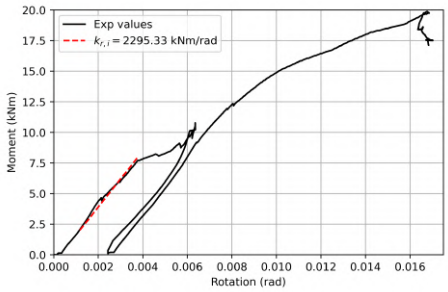

Figure 7: Moment vs rotation behaviour of the joint.

2 Analytical model for capacity

2.1 Model formulation

Experimental results showed that the capacity of WikiHouse floor beams is dominated by the dovetail joint on the side panels (Figure **??**). Specifically, the stitched joints connecting the bottom panel to the side panel failed in compression.

The side panel is divided into 3 parts named 1, 2 and 3 from left to right (Figure 8). Parts 1 and 3 have length equal to a. The total length of the beam is equal to L. The connection between the side panels and the bottom panel is made by stitched joints, also called tabs. Tabs have width equal to w, thickness equal to t and spacing equal to s. The distance between the tabs and the top of the beam is equal to h.

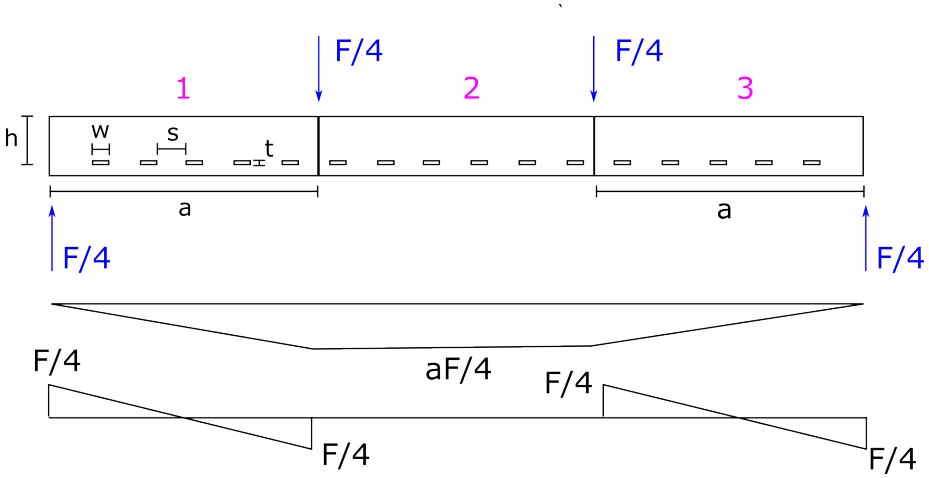

Figure 8: Geometry of the beams, bending moment diagram and shear diagram.

2.2 Force in the tabs

During the test, the beam was subjected to a 4 point bending test with force at the actuator equal to F. The point of application of the forces was on top of the dovetail joint as it can be seen from Figure 4. Since there are two lateral panels in the beam, the force on each dovetail is equal to $F/4$. This leads to the bending moment diagram and shear diagram shown in Figure 8.

The deformed shape of the side panel is schematically reported in Figure 9. The bending contribution of the dovetail joint has been left out for the sake of simplicity.

Imposing the equilibrium of moments on part 1 leads to:

$$\frac{aF}{4} = \sum_{i}^{n_1} F_{T1i} h \tag{1}$$

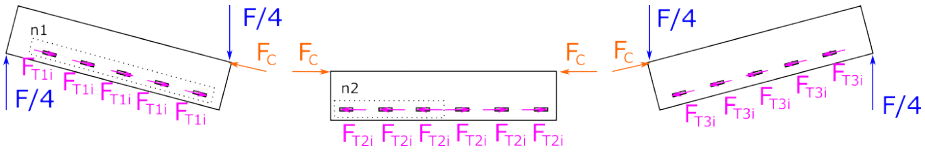

Figure 9: Schematic deformation of the side panels.

with F_{T1i} the force on the i^{th} tab belonging to part 1, and n_1 the number of tabs in part 1.

The contact force between part 1 and part 2 is indicated with F_c. Imposing the equilibrium of forces in the direction of the panel longitudinal axis leads to:

$$F_c = \sum_{i}^{n_1} F_{T1i} = \frac{aF}{4h} \tag{2}$$

Similarly on part 2, the equilibrium of forces leads to:

$$\sum_{i}^{n_2} F_{T2i} = F_c = \frac{aF}{4h} \tag{3}$$

with n_2 half of the number of tabs in part 2 and F_{T2i} the force on the i^{th} tab. Note that half of the tabs in part 2 deal with the contact force coming from part 1, and half deal with the contact force coming from part 3.

Whether the tabs in part 1 or 2 dominate the joint response depends on the number of tabs:

1. if $n_2 < n_1$, then $F_{T2} > F_{T1}$. Hence the tabs in part 2 dominate the joint behaviour.
2. if $n_2 < n_1$, then $F_{T2} > F_{T1}$. Hence the tabs in part 1 dominate the joint behaviour.

2.3 Moment capacity (joint)

The moment capacity of the dovetail joint M_j can be expressed as:

$$\begin{cases} n_2 > n_1 : & M_j = 2n_1 F_t h \\ n_2 < n_1 : & M_j = 2n_2 F_t h \end{cases} \tag{4}$$

with F_t the capacity of a single tab. The factor 2 appears because there are two side panels for each beam.

2.4 Moment capacity (mid-span)

The moment capacity in the mid-span can be calculated following the same logic. According to the forces distribution in Figure 9, the moment capacity in the mid span

$M_{L/2}$ can be calculated as:

$$M_{L/2} = 2n_2F_th \tag{5}$$

with F_t the capacity of a single tab. The factor 2 appears because there are two side panels for each beam.

2.5 Comparison with experimental results

Five M beam specimens and three L beam specimens were tested in 4-point bending. M specimens had a span of 5.1 m (column centre to column centre), and were 350 mm high and 600 mm wide. L specimens had the same section but spanning 5.7 m (column centre to column centre). Tabs were 100 mm wide and the spacing between them was equal to 200 mm. Further geometry details are reported in Figure 10.

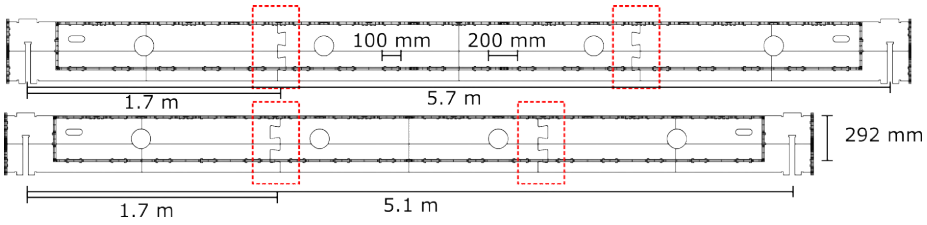

Figure 10: Tested specimens.

The capacity F_t of the tab can be calculated as the minimum between $F_{t,c}$ (compression failure) and $F_{t,s}$ (shear failure):

$$F_t = min(F_{t,c}, F_{t_s}) = min(\overbrace{A_c}^{18\cdot18}\ \overbrace{f_{c,0}}^{24.6}, \overbrace{A_s}^{100\cdot18}\ \overbrace{f_s}^{5.4}) = 8.0\ kN \tag{6}$$

where A_c is the contact area in compression, $f_{c,0}$ is the average compression strength of Metsa plywood parallel to the grain, A_s is the shear area of the tab and f_s the shear strength of Metsa plywood. Note that the average values of the material properties are used in equation 6, and not the characteristic values. This is to compare the model results with the experimental values. Characteristic values should be used for the design.

Results are consistent with what was observed while testing the stitched joint in compression, where the average capacity was found to be equal to 7.5 kN.

Considering n_2 equal to 4 and 3 for the L specimens and M specimens respectively, it leads to the following values of M_j and $M_{L/2}$:

1. L specimens: $M_j = M_{L/2} = 2\overbrace{n_2}^{4}\underbrace{F_t}_{8}\overbrace{h}^{0.292} = 18.7\ kNm$

2. M specimens: $M_j = M_{L/2} = 2\overbrace{n_2}^{3}\underbrace{F_t}_{8}\overbrace{h}^{0.292} = 14.0\ kNm$

Analytical values in terms of moment capacity are 12% and 27% lower than the average experimental values for the L specimens (21.2 kNm) and M specimens (19.0 kNm), respectively. Although simplified, the analytical model seems to provide acceptable and conservative values for design purposes.

3 Analytical model for deflection

3.1 Model formulation

The model is based on Euler-Bernoulli equations, with the addition of a rotational spring at the dovetail joint. Integrating the differential equations (see section 5 for details) leads to the following formula for calculating the vertical displacements:

$$v(x) = \begin{cases} v^{left}(x) = -\frac{F}{6EI}x^3 + [-\frac{Fa^2}{2EI} + \frac{FaL}{2EI} + \frac{Fa}{k_r}]x & x \leq a \\ v^{right}(x) = -\frac{Fa}{2EI}x^2 + (\frac{FaL}{2EI})x + -\frac{Fa^3}{6EI} + \frac{Fa^2}{k_r} & a \leq x \leq 0.5L \end{cases} \quad (7)$$

with E the elastic modulus, I the inertia modulus, a the distance of the dovetail joint from the support, L the span and k_r the rotational stiffness of the joint.

3.2 Comparison with experimental results

The deflection of the beam was calculated by:

1. A traditional beam model (Euler-Bernoulli) without considering the rotational stiffness contribution and considering an elastic second moment of inertia I. This last was calculated by using the geometry of the section, and it resulted equal to $I = 522.7 \cdot 10^6\ mm^4$
2. A traditional beam model (Euler-Bernoulli) + rotational springs ($k_R = 2295\ kNm/rad$) and considering an elastic second moment of inertia.
3. A traditional beam model (Euler-Bernoulli) + rotational springs and considering an effective second moment of inertia (55% of the elastic one)

and compared with the experimental results in Figure 11 and Figure 12.

It was found that:

1. Not considering the joint flexibility (i.e. rotational springs) underestimates the deflection.
2. Using the elastic moment of inertia I_{el} also underestimates the overall deflection.

Hence, it is recommended to take into account the joint flexibility as well as using an effective moment of inertia I_{eff} equal to 55%I_{el} or lower.

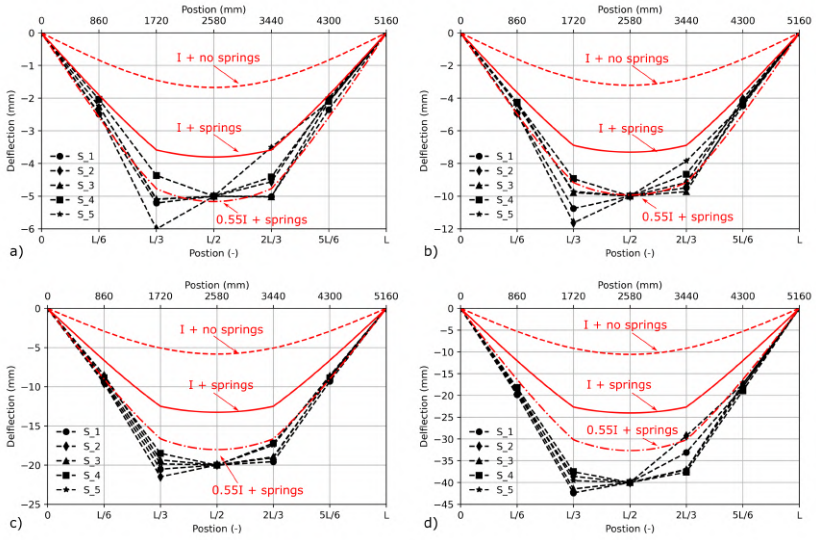

Figure 11: M specimens: experimental vs analytical results.

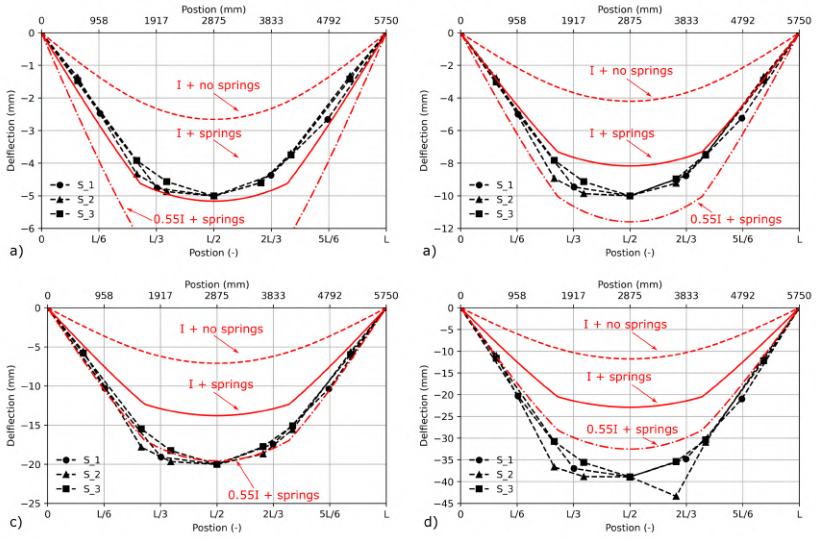

Figure 12: L specimens: experimental vs analytical results.

4 Design of WikiHouse beams

4.1 Design table

A design table for the different geometries available on the WikiHouse website is reported in Table 3 . The geometry of the beams is reported in Figure 13 for the 250 series, and in Figure 14 for the 200 series.

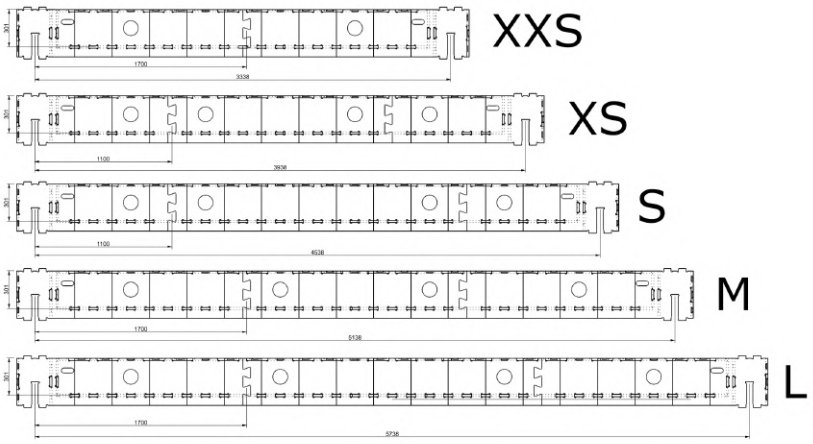

Figure 13: Geometry of the 250 series

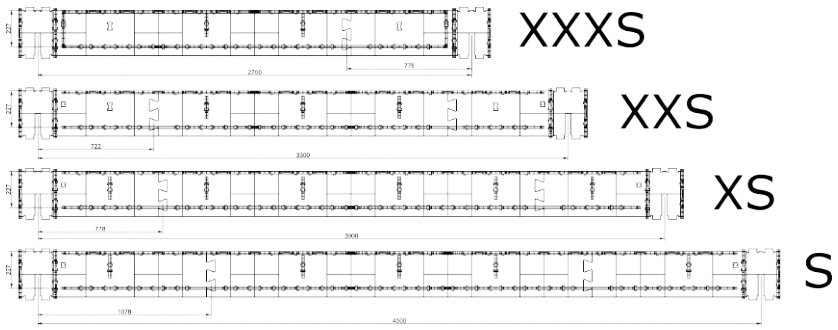

Figure 14: Geometry of the 200 series

For any of the beams in Figure 14 and 13, the following values are provided in Table 3:

1. Series: either 250 or 200.
2. Span in mm (center-column to center-column).
3. Distance of the dovetail joint from the center column, labelled with a.

Table 3: Design table for the 250 and 200 series.

Series	Size	Span (mm)	a (mm)	n_1	n_2	h (mm)	$W_j(mm3)$	$W_{L/2}(mm^3)$	$I(cm^4)$	$k_R(kNm/rad)$
250	XXS	3338	1658	9	9	292	1702944	1702944	28765	2295
	XS	3938	1100	5	5	292	946080	946080		
	S	4538	1100	5	7	292	946080	1324512		
	M	5138	1700	9	5	292	946080	946080		
	L	5738	1700	9	6	292	1135296	1135296		
200	XXXS	2700	778	3	3	218	211896*	283824*	12692	1713
	XXS	3300	726	3	5	218	211896*	473040*		
	XS	3900	786	3	7	218	211896*	662256*		
	S	4500	1080	5	7	218	353160*	662256*		

* Conservative values reduced by 50%.
** Extrapolated value.

4. number of tabs contributing to the moment capacity, labelled with n_1 and n_2 (see Figure 9).

5. Distance between the center of the tabs to the top flange of the beam, labelled with h.

6. Section modulus at the joint W_j. It was calculated as $W_j = 2{\cdot}min(n_1, n_2){\cdot}h{\cdot}t^2$, with $t = 18\ mm$ the thickness of the panel.

7. Section modulus at the mid-span $W_{L/2}$. It was calculated as $W_{L/2} = 2{\cdot}n_2{\cdot}h{\cdot}t^2$, with $t = 18\ mm$ the thickness of the panel.

8. Effective second moment of inertia according to section 3.2.

9. Rotational stiffness of the dovetail joint, see section 1.4.

Note that for the 200 series, two main modifications were introduced. First, the section modulus was conservatively reduced by 50% to compensate the lack of experimental data. Since the section of the 200 series is smaller, a different failure mode could be triggered. Specifically, the tabs in the bottom flange might not reach yielding before the splitting of timber under the tab. This is because the tabs are closer to the edge of the side panel than the 250 series, so there is no evidence that the failure mode will be the same. Second, the flexibility of the dovetail joint k_R was linearly scaled by the ratio of the heights. In other other words:

$$k_{R,200} = \underbrace{\frac{\overbrace{h_{200}}^{218}}{h_{250}}}_{292} \overbrace{k_{R,250}}^{2295} = 1713\ kN/rad$$

4.2 Vertical deflection

While Equation 7 is suitable for the loading condition that the beams experience during testing (Figure 1), it is not of practical use for design purposes. This is because, beams are normally considered subjected to distributed forces in typical design scenarios.

The maximum vertical displacement in the midspan v_{max} of a WikiHouse beam subjected to a distributed load q can be calculated by using equation 8:

$$v_{max} = \frac{5qL^4}{384EI} + \frac{qa^2}{2k_r}[L - a] \tag{8}$$

with E the elastic modulus, I the inertia modulus, a the distance of the castellated joint from the support, L the span and k_r the rotational stiffness of the joint.

Equation 8 was obtained by integrating Euler-Bernoulli equations and introducing a rotational stiffness element in the dovetail joint. The mathematical derivation is reported in section 6.

5 Appendix A: displacement formula for beam with rotational springs and concentrated forces

The vertical deflection $v(x)$ and rotation $\phi(x)$ of the beam can be written a as:

$$\frac{\mathrm{d}^2 v(x)}{\mathrm{d}x^2} = \frac{\mathrm{d}\phi(x)}{\mathrm{d}x} = \frac{-M(x)}{EI} \tag{9}$$

where E is the elastic modulus, I is the modulus of inertia and $M(x)$ is the bending moment function of the position coordinate x (Figure 15).

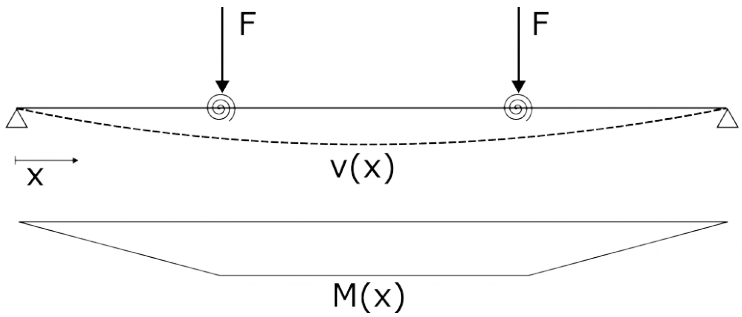

Figure 15: Representation of the structural model and bending moment function.

The bending moment $M(x)$ is expressed by equation 10:

$$M(x) = \begin{cases} Fx & x \leq a \\ Fa & a \leq x \leq 0.5L \end{cases} \tag{10}$$

with a the distance between the point of load application and the support, and L the span. Note that the deflection is symmetric, therefore the problem is studied for $0 \leq x \leq 0.5L$.

Integrating equation 9 and substituting the bending moment function expressed by equation 10 leads to new expression for rotation $\phi(x)$ and vertical deflection $v(x)$, which are presented in equation 11 and equation 12:

$$\phi(x) = \begin{cases} \phi^{left}(x) = -\frac{F}{2EI}x^2 + C_1 & x \leq a \\ \phi^{right}(x) = -\frac{Fa}{EI}x + D_1 & a \leq x \leq 0.5L \end{cases} \tag{11}$$

$$v(x) = \begin{cases} v^{left}(x) = -\frac{F}{6EI}x^3 + C_1 x + C_2 & x \leq a \\ v^{right}(x) = -\frac{Fa}{2EI}x^2 + D_1 x + D_2 & a \leq x \leq 0.5L \end{cases} \tag{12}$$

with C_1, C_2, D_1, D_2 constants of integration. These last be determined by considering the boundary conditions according to equation 13:

$$\begin{cases} v_{(x=0)} = 0 \\ \phi_{(x=0.5L)} = 0 \\ \phi^{left}_{(x=a)} - \phi^{righ}_{(x=a)} = \frac{M_{(x=a)}}{k_r} \\ v^{left}_{(x=a)} = v^{righ}_{(x=a)} \end{cases} \tag{13}$$

with k_r the rotational stiffness of the spring. The boundary conditions express that:

1. the vertical displacement at the support is equal to 0 (because of the support).
2. the rotation in the midspan is equal to 0 (because of the symmetry of the deflected shape).
3. the difference of rotation in correspondence of the rotational spring is proportional to the moment and the spring stiffness.
4. there is no differential vertical displacement in correspondence of the spring (continuity of the element).

Solving the system of equations 13, 11 and 12 allows to determine the following values for the constants of integration:

$$\begin{cases} C_1 = -\frac{Fa^2}{2EI} + \frac{FaL}{2EI} + \frac{Fa}{k_r} \\ C_2 = 0 \\ D_1 = \frac{FaL}{2EI} \\ D_2 = -\frac{Fa^3}{6EI} + \frac{Fa^2}{k_r} \end{cases} \tag{14}$$

6 Appendix B: displacement formula for beam with rotational springs and distributed load

The equation for calculating the maximum displacement ca be obtained by integrating the Euler-Bernoulli equations. Since the spring introduces a discontinuity in the rotation, both rotation $\phi(x)$ and displacement $v(x)$ are need to be written before and after

the discontinuity:

$$\begin{cases} v^{left}(x) = \frac{q}{24EI}x^3 - \frac{qL}{12EI}x^3 + C_1 x + D_1 & x \leq a \\ v^{right}(x) = \frac{q}{24EI}x^3 - \frac{qL}{12EI}x^3 + C_2 x + D_2 & a \leq x \leq 0.5L \end{cases} \tag{15}$$

$$\begin{cases} \phi^{left}(x) = \frac{q}{6EI}x^3 - \frac{qL}{4EI}x^2 + C_1 & x \leq a \\ \phi^{right}(x) = \frac{q}{6EI}x^3 - \frac{qL}{4EI}x^2 + C_2 & a \leq x \leq 0.5L \end{cases} \tag{16}$$

where E is the elastic modulus, I is the modulus of inertia and $M(x)$ is the bending moment function of the position coordinate x (Figure 16).

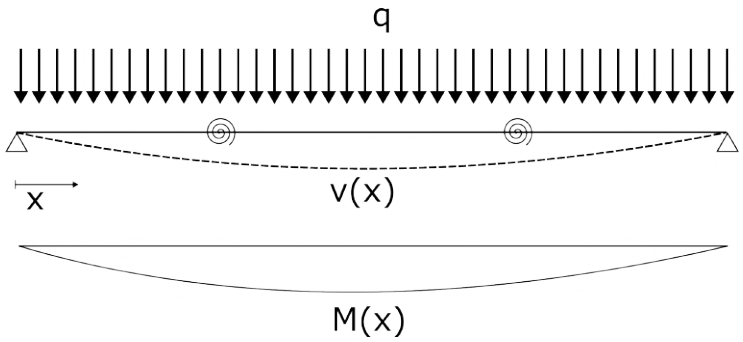

Figure 16: Representation of the structural model and bending moment function.

The value of the integration constants C_1, C_2, D_1, D_2 can be found by imposing the following boundary conditions:

$$\begin{cases} v^{left}(0) = 0 \\ \phi^{right}(L/2) = 0 \\ \phi^{right}(a) - \phi^{left}(a) = \frac{M(a)}{k_r} \\ v^{left}(a) = v^{right}(a) \end{cases} \tag{17}$$

The physical meaning is that:

1. the vertical displacement at the left support is 0
2. the rotation at the midspan is equal to 0 (the beam is symmetric)
3. the difference of rotation in correspondence of the castellated joint is proportional to the bending moment divided by the rotational stiffness of the joint
4. the vertical displacement in $x = a$ is continuous.

By substituting eq. 17 into eq. 15 and eq. 16, the values of the integration constants can be calculated:

$$\begin{cases} D_1 = 0 \\ C_2 = \frac{qL^3}{24EI} \\ C_1 = \frac{qL^3}{24EI} + \frac{qa}{2k_r}[L-a] \\ D_2 = \frac{qa^2}{2k_r}[L-a] \end{cases} \tag{18}$$

Acknowledgements

The series of experiments was carried out at the University of Edinburgh. The contribution of Tom Reynolds, Rafik Taleb and the technical staff in the structural engineering lab is greatly appreciated.

References

[1] CEN. *BS EN 1380:2009 Timber structures. Test methods. Load bearing nails, screws, dowels and bolts*. 2009.